

LETTER • OPEN ACCESS

Distribution of small seasonal reservoirs in semi-arid regions and associated evaporative losses

To cite this article: Bassem Mady *et al* 2020 *Environ. Res. Commun.* **2** 061002

View the [article online](#) for updates and enhancements.

Environmental Research Communications

**OPEN ACCESS****LETTER**

Distribution of small seasonal reservoirs in semi-arid regions and associated evaporative losses

RECEIVED
24 January 2020**REVISED**
26 April 2020**ACCEPTED FOR PUBLICATION**
13 May 2020**PUBLISHED**
3 June 2020**Bassem Mady**¹ , **Peter Lehmann**¹ , **Steven M Gorelick**² , **Dani Or**¹ ¹ Department of Environmental Systems Science, ETH Zurich, Zurich, Switzerland² School of Earth, Energy and Environmental Sciences, Stanford University, CA, United States of AmericaE-mail: bassem.mady@usys.ethz.ch**Keywords:** small reservoirs, semi-arid, seasonal water storage, water resources monitoring, floating covers, evaporation suppression, dry season evaporationSupplementary material for this article is available [online](#)

Original content from this work may be used under the terms of the [Creative Commons Attribution 4.0 licence](#).

Any further distribution of this work must maintain attribution to the author(s) and the title of the work, journal citation and DOI.

**Abstract**

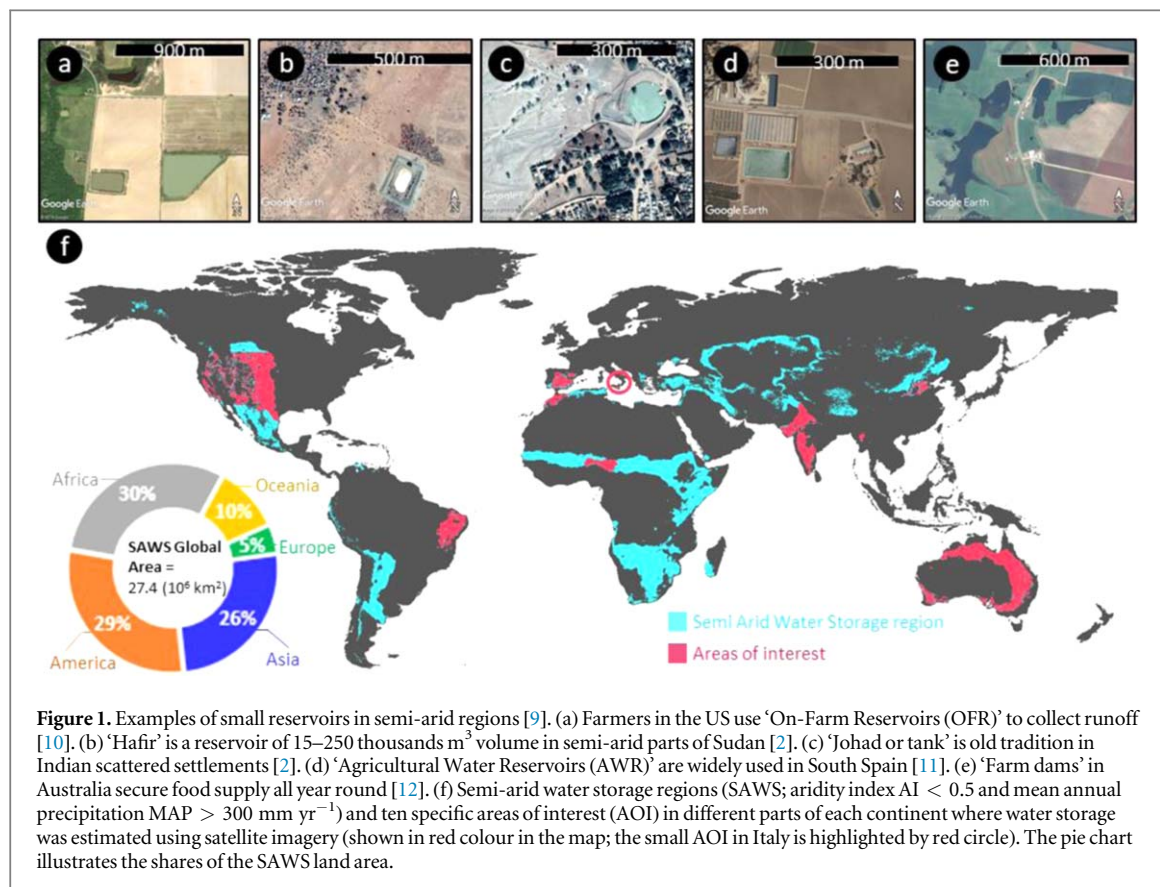
To support the increasing demand of a growing population for freshwater, small-sized ($<0.1 \text{ km}^2$) water reservoirs are necessary in areas with limited infrastructure, especially in water-stressed regions having seasonal and variable precipitation. Seasonal storage in small reservoirs is often overlooked in present inventories. Accordingly, we assessed the current state in semi-arid regions using highly resolved Sentinel-2 satellite imagery. Globally, about 3 million small reservoirs are in operation in semi-arid regions having a total water surface area of $17\,800 \text{ km}^2$ and seasonal storage of 37 km^3 , supporting 15% of the world's population in semi-arid regions. Estimated upper-bound of evaporative losses represent 38% (14 km^3) of storage during dry season. The study estimates the evaporation suppression using floating covers and lays foundation to assess the feasibility of this technical solution to increase water savings.

Significance and originality statement

This study provides new insights into the distribution of seasonal freshwater storage in water stressed regions that support large rural population. We provide the first baseline dataset of this distributed freshwater resource to better assess the sustainability of communities in semi-arid regions with chronic water shortages. Water storage in semi-arid regions is subject to potential evaporative losses of nearly 40% of the stored water. We analyzed conditions where evaporative losses could be significantly reduced using floating covers, a simple and scalable solution suitable for regions with underdeveloped economies. The study as well ranks regions with highest potential benefits from evaporation suppression measures.

1. Introduction

The long tradition of freshwater storage in reservoirs to meet dry-season needs is likely to expand due to the increasing water demand for food production, in a changing climate of a rapidly growing human population [1]. Small seasonal reservoirs have been used in different regions of the world for centuries, especially in semi-arid regions (known under different local names [2, 3], see figures 1(a)–(e)). In these regions, dry-season water shortages for agricultural livelihood are common and water storage remains a feasible mitigation measure, while more recently, additional off-grid electric power supply was facilitated by means of micro-dams [4, 5]. In contrast with well-studied large reservoirs and dams, small-sized and seasonal freshwater storage systems have relatively low environmental impact [6], yet their distribution and function during dry seasons plays a critical role in promoting the sustainability of rural communities and farmers, and reduce societal inequality gaps [7] for 15% of the world's population inhabiting semi-arid regions [8].



The significance of dry-season water scarcity in rural semi-arid regions with limited infrastructure goes beyond the water value in terms of costs of alternate water sources. It determines the number of livestock that can be supported or the severity of staple crop yield losses [13]. Water shortages have amplified from 6% to 35% between 1960 to 2005, and the gap continues to expand with population growth especially in Southern Asia [14]. Systematic socio-economic analyses of seasonal rainwater harvesting methods have concluded that open water reservoirs and sand dams with capacities of 100 to 10 000 m^3 are the most efficient (0.04–0.4 USD m^{-3}) due to their longer lifetime [15]. However, in some basins it has been shown that river discharge could be impacted by uncontrolled construction of farm dams, especially in the absence of regulation for reservoir filling periods [6, 16]. At present, in some catchments the density of such small reservoirs may reach 10 reservoirs per km^2 [16], yet a systematic assessment of the global distribution of such an important class of small reservoirs remains lacking. With development of remote sensing techniques for retrieving salient information from satellite imagery [17–19], the identification of locations, sizes, and usage of small water reservoirs now becomes feasible.

Globally, freshwater storage is distributed predominantly in temperate and cold climates where a few large reservoirs dominate the regional storage. The nature of reservoir size and number distributions suggest power-law relations where the number of small reservoirs far exceeds that of large ones [20]. Estimates based on global data sets [21, 22] show that 1.8% of land area is covered by reservoirs and large lakes, however, these values omit small reservoirs (<0.1 km^2 that are the core of this study) and the gaps to this point are primarily addressed by extrapolation of size distribution models [18]. Based on a number of surveys in a few regions of the world, Downing *et al* [23] estimated that small impoundments and farm reservoirs account for up to 1.2% of global land area.

The characteristics of small seasonal reservoirs, i.e., freshwater bodies with an area <0.1 km^2 , vary across regions reflecting geomorphological, climatic and social factors [24–26] (see figures 1(a)–(e)). A comprehensive dataset (Hydrolakes) lists 1.42 million freshwater reservoirs and storage lakes with 182 000 km^3 total storage [19]. Hydrolakes dataset considers storage reservoirs and dams with volumes larger than 0.1 km^3 including 6 862 reservoirs previously reported in a related dataset (GRanD [27]). Both global datasets neglect local (on-farm or village) small reservoirs (<0.1 km^2) that are crucial to rural communities with chronic seasonal water shortages, limited infrastructure and often lacking alternate water sources. This omission of small reservoirs is pervasive in other global studies of inland water bodies, often attributed to resolution limits of satellite products, such as MODIS [28] and Landsat [29, 30] with spatial resolutions of 250 and 30 m, respectively.

Advanced satellite imagery at 10 m resolution (Sentinel-2) permits bridging this gap to provide regional estimates of the numbers, sizes and spatial distributions of small water reservoirs ($<0.1 \text{ km}^2$) in semi-arid regions. These highly stressed regions are home for approximately one billion people, typically living in rural communities under conditions of chronic water shortages. The high evaporative demand in these regions results in 20 to 50% loss of the stored water [12, 31]. In this study, we aim to estimate potential evaporative losses from small reservoirs in different semi-arid regions of the world, and assess the potential of reducing evaporative losses using floating covers [12, 32, 33]. The specific objectives of this study were to: i) quantify the numbers and sizes of small water reservoirs in semi-arid regions globally, and ii) estimate evaporative losses and potential of evaporation suppression measures, considering climatic conditions in each region.

2. Materials and methods

2.1. Identification of study regions

To quantify the size and density of small water reservoirs and estimate associated evaporative losses, we selected regions where water is seasonally scarce, yet rainfall is predictably sufficient to fill water reservoirs. Our study focuses on semi-arid regions (prone to high evaporation losses) where seasonal rainfall ($800 \text{ mm} > \text{mean annual precipitation (MAP)} > 300 \text{ mm}$) as delineated in figure 1(f). The mean annual aridity index (ratio of precipitation to potential evapotranspiration) $\text{AI} < 0.5$ [34, 35] was estimated from 1950 to 2000, and $\text{MAP} > 300 \text{ mm}$ for the record from 1979 to 2013 [36]. We filtered out regions that preclude the use of reservoirs, such as forests, urban areas, wetlands, and mountains using consistent global land cover (300 m pixel size) ESA products [37].

Within this region (called semi-arid water storage region, SAWS), we selected 10 specific ‘areas of interest’ (AOI) where—(i) different forms of agriculture are taking place, and (ii) water storage could be practiced. The 10 AOI cover a range of socio-economic states, agricultural practices, and infrastructure potential conditions (for assessing alternate water sources and evaporation suppression value) across five continents focusing on USA, Brazil, Spain, Italy, Morocco, Nigeria, India, Myanmar, China, and Australia as representative countries.

2.2. Small reservoirs detection

The AOI is overlain by a $10 \times 10 \text{ km}$ grid with 10% of grid cells (a grid cell is denoted in the following as a ‘mask’—see SI, figure S1 is available online at stacks.iop.org/ERC/2/061002/mmedia) randomly chosen to quantify water reservoir size and spatial density from the relevant Sentinel-2 satellite imagery within each mask (the sampling percentage choice of 10% of the AOI is explained in SI—figure S2). The Satellite captures 13 different wavelength bands ($443 \text{ nm}–2190 \text{ nm}$) with pixel size of 10–60 meters (depending on wavelength; see SI, table S1). As we show in more detail in Supplementary Information file (figure S9), the reflectance (measured by satellite) in the infrared range is much smaller compared to soil and vegetation and can reasonably distinguish water bodies.

We used imagery acquired at the end of the wet season (see SI, figure S6 for the distinction between wet and dry seasons) assuming that most reservoirs are water filled—this is marked as time T_0 . Another image for the same area is acquired 90 days later in the dry season (T_{val}) to provide quality check and avoid randomly inundated lands (only areas also classified as ‘water’ after 90 days are considered as water reservoirs). To classify water reservoirs, inundated agricultural land (e.g., rice) and vegetation, we have used two indices; Normalized Difference Water Index NDWI (positive for water areas but negative for other surfaces), and Normalized Difference Vegetation Index NDVI (positive for vegetation) that were computed at T_0 and T_{val} . Region-specific thresholds were defined for NDWI and NDVI to extract binary images for vegetation and initial water bodies (see SI, section 1 and figure S1).

2.3. Power-law frequency-magnitude distribution

Results of previous inventories of large reservoirs and natural lakes [38] show that the frequency-size distribution follows a power-law. As presented in figure 2(b), a power-law distribution was fitted for our data of small water reservoirs (5 size classes) truncating areas above $100 000 \text{ m}^2$ (0.1 km^2) and those below 300 m^2 as well to reduce the bias that can be introduced to the fitted power-law exponent (decrease in the absolute value of β) with the detection failure of reservoirs at the satellite imagery cell limit ($100–200 \text{ m}^2$). We bin the frequency of reservoirs that fall in 5 size classes since the reservoirs have irregular shapes and might not be filled to top at time of image acquisition; hence the exact area of the reservoir could have some discrepancies particularly because a rather conservative NDWI threshold is applied. The power-law is determined by computing the probability density function (pdf) for the reservoir sizes extracted from the masks:

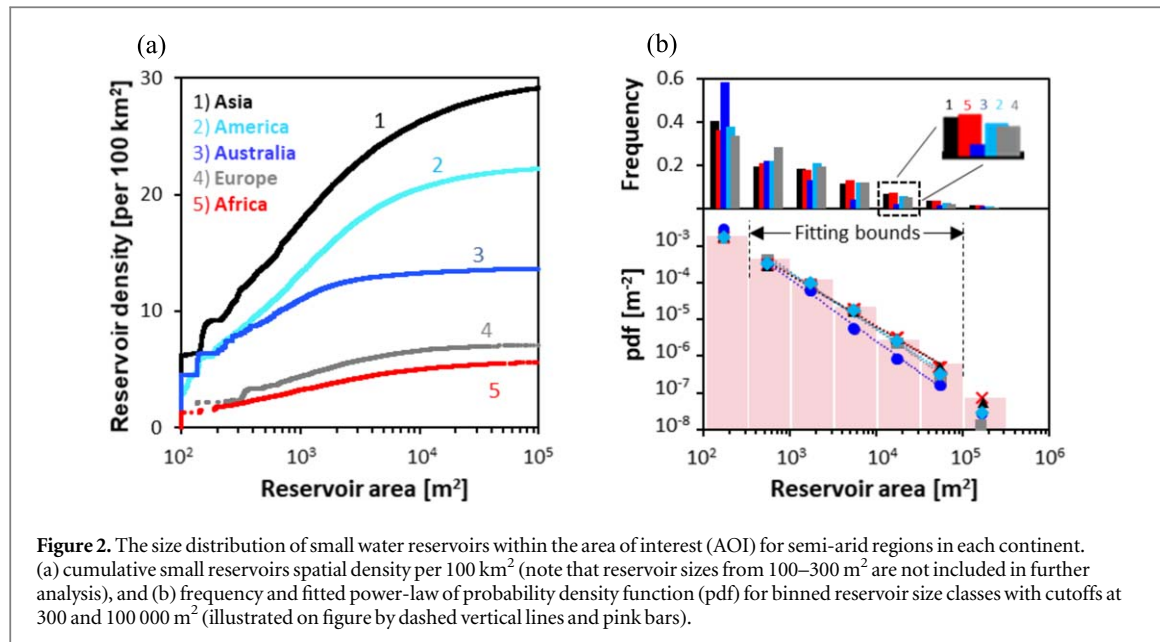


Figure 2. The size distribution of small water reservoirs within the area of interest (AOI) for semi-arid regions in each continent. (a) cumulative small reservoirs spatial density per 100 km² (note that reservoir sizes from 100–300 m² are not included in further analysis), and (b) frequency and fitted power-law of probability density function (pdf) for binned reservoir size classes with cutoffs at 300 and 100 000 m² (illustrated on figure by dashed vertical lines and pink bars).

$$pdf(A) = K \cdot A^\beta \quad (1)$$

with reservoir area A , coefficient K and power-law exponent β . To estimate the total storage in the SAWS (AOI in addition to blue area in figure 1(f)), we first aggregated all water reservoirs from the different AOIs by continent (note that in the remaining text ‘Oceania’ is referred to as ‘Australia’ due to the lack of SAWS in other parts of that geographic region), then derived power-laws for each continent (see SI—table S2) scaled for reservoir density per km² and size. The differences reflect effects of climate and anthropogenic practices in different regions of the world since abundance of natural lakes in semi-arid regions is marginal [23].

To estimate number and volume of reservoirs, we assign a representative size to each of the five size classes (‘bins’) that were used to determine the power-law (see figure 2(b)). The estimated number of reservoirs within a size class of areas ΔA defined by maximum a_{\max} and minimum area a_{\min} was then calculated as:

$$N_{a_{\min} < A \leq a_{\max}} = M \cdot K \cdot A^\beta \cdot \Delta A \quad (2)$$

with area M of SAWS per continent in km² and the area A in m² representative for the size class defined by:

$$A = 10^{0.5(\log(a_{\max}) + \log(a_{\min}))} \quad (3)$$

Studies have shown that reservoir volume is related to its surface area by power function whose parameters may vary spatially [24, 39]. We synthesized several reported power-laws linking reservoir area and volume into a representative relation which includes the regional differences (see SI, section 2). The relation enables estimation of the stored water volume (V , m³) from observed reservoir area (A , m²) (see SI, figure S3) using:

$$V = 0.38 A^{1.173} \quad (4)$$

To estimate the water storage per SAWS for each continent, we estimate the volume of reservoirs within a size class of representative area A with density N simply as:

$$V_{a_{\min} < A \leq a_{\max}} = 0.38 \cdot N \cdot A^{1.173} \quad (5)$$

3. Results and discussion

3.1. Inventory of small water reservoirs in semi-arid regions

We estimate small reservoir numbers and storage capacity in semi-arid regions (about 27 million km²—21% of the Earth land surface). The number and areas of small water reservoirs were estimated by spatial sampling of 4770 masks (each covering 100 km²) randomly distributed over 10% of the representative AOI (red regions in figure 1(f)). The spatial density of small reservoirs varied across regions (SI, table S3) with highest density of 420 reservoirs in a sampling mask in South Asia (India). The lowest average spatial density per country was 5 small reservoirs per 100 km² in Nigeria, and the highest was in Myanmar with 40 small reservoirs per 100 km². The probability density function of reservoir sizes obtained for size classes between 0.0003 and 0.1 km² in SAWS of each continent followed a power-law (see equation (1) in section 2) with similar exponents near 1.5 irrespective

Table 1. The estimated storage and computed evaporation losses of small reservoirs in the semi-arid water storage region (SAWS, blue and red area in figure 1(f)) of each continent for this study.

Continent	Mean rainfall in SAWS (mm yr ⁻¹)	Evaporative demand (ET ₀ , mm yr ⁻¹)	Estimated no. of reservoirs (10 ³)	Estimated area of reservoirs (km ²)	Estimated storage (km ³)	Evaporation losses (%)	Evaporation losses (km ³)
America	529	1750	1136	6167	13.7	31	4.2
Europe	444	1343	60	267	0.5	23	0.12
Asia	477	1574	1217	8695	16.5	39	6.5
Australia	540	2400	156	569	1.2	53	0.63
Africa	600	2317	294	2111	4.8	52	2.5
Global (SAWS)	520	1875	2863	17 809	37	38	13.95

Note: the mean rainfall and evaporative demand (ET₀) is the annual average for the whole semi-arid region in each continent. The estimations are computed using equations (2), (5) for reservoir sizes between 300 and 100 000 m², and the cumulative evaporation losses are represented (i) as percentage of the estimated storage per continent and (ii) as volume per dry season.

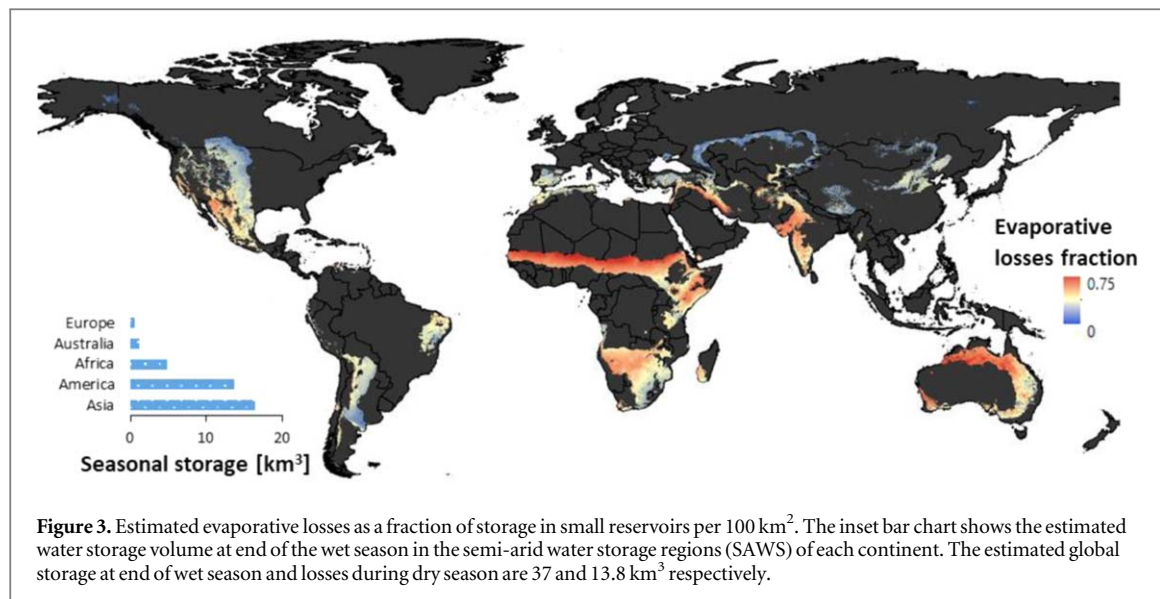
of climate and population density, as depicted in figure 2. Additional information on the sensitivity of the power-law coefficients to the sampling procedure and reservoir extraction accuracy are provided in SI—figures S2 and S4, respectively. The number and area of small water reservoirs for the entire SAWS of each continent were deduced from the estimated power-laws as represented in figure 2(b), and water storage volumes from area-volume relations (see equation (4) in section 2). The median small-reservoir size was $\sim 1\ 400\ m^2$ with Australia tending to have smaller reservoirs, and the largest in Africa and America. As reported in table 1, we estimated 2.9 million small reservoirs globally in the SAWS with an estimated total water surface area of 17 800 km² and seasonal storage of 37 km³.

We examined the potential of extending power-law distributions of size-densities for large reservoirs from other studies to recover the small-reservoir results of this study. For a direct comparison, we first estimated power-law relations for the size distribution of large lakes or reservoirs (Hydrolakes and GRaND) restricted to the SAWS in each continent [19, 27]. The extrapolated estimates using large water bodies relations exhibited significant discrepancies with the direct estimates of small reservoirs size-density (see SI, figure S5(a) and table S2). In addition, we found that the approach proposed by Downing *et al* [23] for estimating farm ponds from the area of farmlands (within administrative boundaries; e.g. cities) and mean annual precipitation tends to overestimate reservoirs coverage as shown in SI (figure S5(c)) for an example in entire SAWS of India. The discrepancy could be attributed to the climatic differences as their field surveys were conducted primarily in humid regions of the USA. Finally, we assessed whether the size-density distribution of small reservoirs in SAWS, primarily in the USA, was similar to that obtained for natural lakes and reservoirs of same size range in humid northern regions. The resulting size-frequency distribution of natural lakes with areas between 0.0003 and 0.1 km² delineated from Sentinel-2 imagery followed a power-law with an exponent of 1.2 (see SI, figure S5(b)) and was significantly lower than exponent of 1.8 for water reservoirs in semi-arid regions. The total water surface area per 100 km² for natural small lakes was 25% less than for small water reservoirs in semi-arid regions. These results suggest that resulting small-reservoir size distributions carry signatures of anthropogenic construction practices and differences in climatic conditions.

3.2. Estimated evaporation losses from small water reservoirs

Water losses from small reservoirs in semi-arid regions are attributed primarily to evaporation [40]. Seepage losses are negligible considering that on-farm ponds are often lined by low-permeability clay liners, plastic sheets or sprayed concrete [2, 41]. An objective of this study was to capitalize on the estimated small-reservoir distribution to assess the efficacy of methods for suppressing evaporation in their regional context. We thus estimate the regional evaporation demand considering regional climate and seasonal storage.

While direct measurements of open water evaporation are scarce in semi-arid regions, Penman-Monteith equation (see SI, section 2.2) was proven to provide relatively good estimates for evaporation from open water showing low sensitivity to parameter variations compared to other methods [12, 40, 42, 43]. The evaporative budget (ET^{*}) from free water surfaces of small reservoirs was computed for each region by subtracting the mean monthly precipitation (P) from the cumulative monthly evaporation (ET₀) computed with standard FAO application of the Penman-Monteith method [44] reported in CGIAR dataset [34] (see SI, figure S6(B)) [35]. The estimates focused on the dry period, when evaporative rates are highest and reservoir inflows are negligible. The global precipitation dataset Chelsa [36] was used to identify the dry period for each region within the prescribed SAWS. The months with rainfall values lower than 30% of the maximum monthly precipitation for the northern



and southern hemispheres were considered as 'dry season' (for equatorial regions the threshold was 50%; see SI—figure S6(A)).

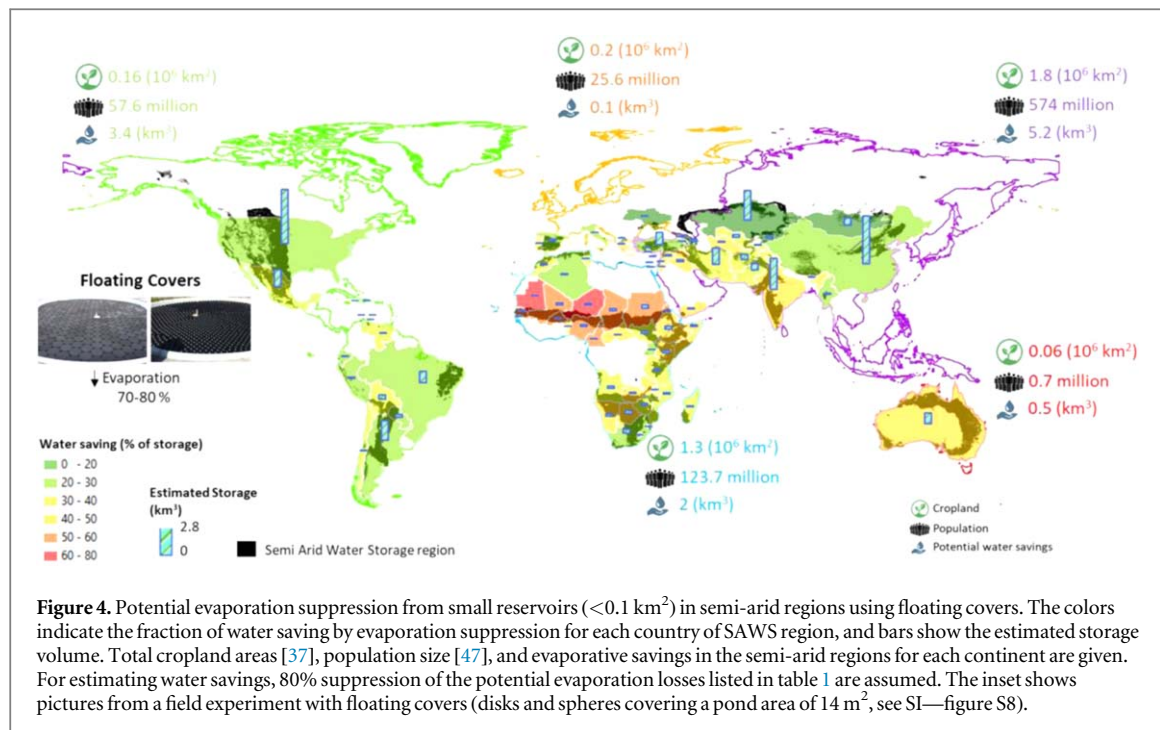
For the computation of the volume losses, we considered a unified geometry for the reservoirs (see SI, section 2.2 and figure S3). During the dry season, the diminishing water depth and shrinking evaporating surface area are calculated based on this unified geometry. The results in figure 3 show that estimated evaporative losses (i) may amount up to 75% of stored water during the dry season, and (ii) vary with regional climate. Note that these estimates represents the upper bound of losses since it neglect the withdrawal of water for water use. When the sum of evaporation and withdrawal during the wet season is larger than the stored volume, the fraction of evaporation to stored volume is slightly different (especially for sizes $>3000 \text{ m}^2$). This is discussed in Supplementary Information file (section 3.1 and table S5).

The fraction of estimated evaporative water losses ranges from 5%–10% in northern latitudes to 75% in the Sahel region and in Australia due to the reception of higher solar radiation in the latter regions. In terms of absolute volumetric water losses (see SI, figure S7), the highest losses were in America and Asia due to high reservoir densities (figure 2(a)). The estimated losses amount to about 38% (13.8 km^3) of the storage during the dry season in the SAWS, while globally the evaporative budget of large dams and artificial reservoirs accounts for only 5% of total storage as reported by Aquastat [45]. Hence, the need for evaporation protection for seasonal small reservoirs in semi-arid regions is acute and should be given attention as discussed in next sub-section.

3.3. Evaporation suppression using floating covers—water saving potential

Cheap floating cover elements could be a simple and scalable solution for suppressing evaporative losses from the many small reservoirs that serve largely rural populations in semi-arid regions. Results from recent studies have shown that across a wide range of climatic conditions, such covers suppress between 70 and 85% of the evaporation relative to uncovered water surfaces [33, 46]. Floating covers reduce the exposed water surface, increase the effective boundary layer over the surface, and shift radiation and heat exchange from the water surface to the top surfaces of the covers [33, 46]. The packing of floating spheres or discs permit light penetration and gas exchange through the 9% uncovered area (gaps formed between the elements), thus permitting ecological functions (we report preliminary results from an ongoing field experiment in SI—section 3 and figure S8). Attractive features of this technologically simple evaporation suppression method are (i) the relatively low cost (SI—section 4), and (ii) the scalability to various reservoir sizes, particularly suitable for small on-farm reservoirs.

The cover effectiveness is influenced by atmospheric conditions [46], but for simplicity we have used a constant evaporation suppression efficiency of 80% over the dry season as specified by Aminzadeh *et al* [33] for Styrofoam disks. In figure 4, we add regional context by presenting savings percentage for each country of SAWS and highlighting social information about the population and agricultural land areas in each continent. Figure 4 reveals that the highest suppression potential is in the Sahel region. However, such ranking may differ considering the economic value of an alternative water source (see SI—section 4). For example, the rank of Australia in the list of suppression potential may decline considering seawater desalination price (due to proximity of SAWS region to the coast and the generally flat topography, the transport of desalinated water may be cheaper than buying floating covers).



4. Summary and conclusion

We provide new global estimates of the spatial distribution and storage capacity of small water reservoirs (0.0003 to 0.1 km^2) in semi-arid regions using high-resolution multi-spectral Sentinel-2 imagery. The resulting small-reservoir densities follow remarkably similar power-law frequency-size relationships, with exponent values close to those of large natural lakes and big reservoirs reported in existing databases (Hydrolakes/GRanD). Despite the exponent values' similarity, we found that the information gap on small reservoirs cannot be extrapolated from existing large dams and lakes data due to the significant difference in spatial densities of small compared to large reservoirs. Hence, for the first time, our study provides reliable estimates of water storage for small reservoirs and enables the estimation of maximum evaporative losses and evaporation suppression potential using floating covers. The water storage in small reservoirs can be characterized as follows:

- The total number of small reservoirs in semi-arid regions is about 2.9 million with a water surface area of 17.8 thousand km^2
- The spatial distribution and areal density of small reservoirs vary significantly (0 to 420 reservoirs per 100 km^2)
- The global seasonal storage in semi-arid regions is about 37 km^3
- Compared to total freshwater reservoirs, the storage in small water reservoirs is small; nevertheless, small reservoirs have a high socio-economic value due to their high density (250 l/capita/dry day for 1 billion people in semi-arid regions)
- The estimated evaporative losses during the dry season may amount up to 38% of total storage (13.8 km^3 losses from 37 km^3 storage) depending on regional climate
- Floating covers could suppress 70%–85% of the evaporative losses

These important and spatially distributed seasonal freshwater storage reservoirs are essential for a significant fraction of the global population (mostly rural) that live in regions with chronic water shortages. The new inventory of small reservoirs enables estimates of seasonal water storage and evaporation losses that are regionally referenced. This information could be of great importance for governments or international organizations to better assess the sustainability of large rural communities in semi-arid regions. It can be utilized for instance to quantify the economic potential of evaporation suppression using floating covers, considering the local climate and infrastructure (see preliminary analysis in SI, section 4).

Acknowledgments

This work was supported by funding provided by the Swiss National Science Foundation (SNSF; project Nr. 200021_172493). S.M. Gorelick was supported by the Belmont Forum Sustainable Urbanisation Global Initiative (SUGI)/Food-Water-Energy Nexus theme via the US National Science Foundation under grant ICER/EAR-1829999 to Stanford University. Any opinions, findings, and conclusions or recommendations expressed in this material do not necessarily reflect the views of these funding organizations. We thank the organizations and scholars that made their data publically available (Sentinel-2 Satellite imagery, and Grand/Hydrolakes global databases, ESA land cover maps), which we used in the reservoir quantification and comparisons.

Data availability

The data that support the findings of this study, as well as the data layers used for the sampling procedure sensitivity checks are available at repository: '<https://figshare.com/s/c258f1894088eaff7ff0>'. All the external datasets that have been used are referenced in the text.

Code availability

The code used for the probability function fitting, reservoir spatial coverage estimation, and sampling procedure sensitivity checks is available at repository: '<https://figshare.com/s/c258f1894088eaff7ff0>'.

Author contributions

B M, P L and D O led the study. B M designed and implemented the computation algorithms, processed the data, and assembled the database. P L and B M performed the data analyses. B M wrote the first draft of the manuscript. P L and D O edited the manuscript. D O and S G revised the manuscript and made significant contributions to the data interpretation. P L, D O and S G read and approved the final version of the manuscript.

ORCID iDs

Bassem Mady  <https://orcid.org/0000-0002-1421-1197>
Peter Lehmann  <https://orcid.org/0000-0003-0051-5066>
Steven M Gorelick  <https://orcid.org/0000-0003-2486-1318>
Dani Or  <https://orcid.org/0000-0002-3236-2933>

References

- [1] Bhuiyan S I and Zeigler R S 1994 On-farm rainwater storage and conservation system for drought alleviation: issues and challenges *On-Farm Reservoir Systems for Rainfed Ricedlands* (Philippines: IRRI)
- [2] Payen J, Faurès J M and Vallée D 2012 Small reservoirs and water storage for smallholder farming: the case for a new approach *AWM Business Proposal Document, AgWater Solutions. Int. Water Mgt. Inst. (IWMI)* pp 44–49
- [3] Enfors E I and Gordon L J 2008 Dealing with drought: the challenge of using water system technologies to break dryland poverty traps *Glob. Environ. Change* **18** 607–16
- [4] Paish O 2002 Small hydro power: technology and current status *Renew. Sustain. Energy Rev.* **6** 537–56
- [5] Berhane G, Gebreyohannes T, Martens K and Walraevens K 2016 Overview of micro-dam reservoirs (MDR) in Tigray (northern Ethiopia): challenges and benefits *J. of Afr. Earth Sci.* **123** 210–22
- [6] Murray-Darling Basin Commission 2008 *Mapping the Growth, Location, Surface Area and Age of Man Made Water Bodies, Including Farm Dams, in the Murray-Darling Basin* (Canberra: Murray-Darling Basin Commission) MDB Publication, (48/08)
- [7] Balazs C 2006 Rural livelihoods and access to resources in relation to small Reservoirs: a study in Brazil's Preto River Basin *Energy and Resources Group* Uni. of California Berkeley
- [8] Safran U N and Adeel Z 2005 Dryland systems *Ecosystems and Human Well-being: Current State and Trends* ed R Hassan, R Scholes and N Ash vol 1 (Washington, D.C., United States: Island Press) 22 623–62
- [9] 2018 Google earth V 7.3.2.
- [10] Yaeger M A, Reba M L, Massey J H and Adviento-Borbe M A A 2017 On-farm irrigation reservoirs in two Arkansas critical groundwater regions: a comparative inventory *Applied Eng. in Agr.* **33** 869–78
- [11] Alvarez V M, Leyva J C, Valero J M and Górriz B M 2009 Economic assessment of shade-cloth covers for agricultural irrigation reservoirs in a semi-arid climate *Agr. water mgt.* **96** 1351–9
- [12] Craig I, Green A, Scobie M and Schmidt E 2005 *Controlling Evaporation loss From Water Storages* (Queensland, Australia: NCEA Publication No. 1000580/1)
- [13] Battisti D S and Naylor R L 2009 Historical warnings of future food insecurity with unprecedented seasonal heat *Science* **323** 240–4
- [14] Kummu M, Ward P J, de Moel H and Varis O 2010 Is physical water scarcity a new phenomenon? Global assessment of water shortage over the last two millennia *Enviro. Res. Letters* **5** 034006

[15] Lasage R and Verburg P H 2015 Evaluation of small scale water harvesting techniques for semi-arid environments *J. of Arid Enviro.* **118** 48–57

[16] Nathan R, Jordan P and Morden R 2005 Assessing the impact of farm dams on streamflows: I. Development of simulation tools *Australasian J. of Water Res.* **9** 1–12

[17] Habets F, Molénat J, Carluer N, Douez O and Leenhardt D 2018 The cumulative impacts of small reservoirs on hydrology: a review *Science of the Total Environment*, **643** 850–67

[18] Chao B F, Wu Y H and Li Y S 2008 Impact of artificial reservoir water impoundment on global sea level *Science* **320** 212–4

[19] Messager M L, Lehner B, Grill G, Nedeva I and Schmitt O 2016 Estimating the volume and age of water stored in global lakes using a geo-statistical approach *Nature Com.* **7** 13603

[20] Schuiling R D 1977 Source and composition of lake sediments *Interaction Between Sediments and Fresh Water. Proc. of an int. Symp. Held at Amsterdam* ed H L Golterman (the Netherlands, September 6–10) pp 12–8

[21] Wetzel R W 1990 Land-water interfaces: metabolic and limnological regulators *Int. Verein. Theor. Limnol. Verh.* **24** 6–24

[22] Meybeck M 1995 Global distribution of lakes ed A Lerman, D M Imboden and J R Gat *Phys. and Chem. of Lakes* (Berlin: Springer) pp 1–35

[23] Downing J A *et al* 2006 The global abundance and size distribution of lakes, ponds, and impoundments *Limnol. Oceanogr.* **51** 2388–97

[24] Thompson J C 2012 *Impact and Management of Small Farm Dams in Hawke's Bay* Victoria University of Wellington New Zealand

[25] Hughes D A and Mantel S K 2010 Estimating the uncertainty in simulating the impacts of small farm dams on streamflow regimes in South Africa *Hydrological Sci. J.* **55** 578–92

[26] Malveira V T C, Araújo J C D and Guntner A 2011 Hydrological impact of a high-density reservoir network in semiarid northeastern Brazil *J. of Hydrologic Eng.* **17** 109–17

[27] Lehner B *et al* 2011 High-resolution mapping of the world's reservoirs and dams for sustainable river flow management *Frontiers in Ecology and the Env.* **9** 494–502

[28] Carroll M L, Townshend J R, DiMiceli C M, Noojipady P and Sohlberg R A 2009 A new global raster water mask at 250 m resolution *Int. J. of Digital Earth* **2** 291–308

[29] Feng M, Sexton J O, Channan S and Townshend J R 2016 A global, high-resolution (30-m) inland water body dataset for 2000: first results of a topographic–spectral classification algorithm *Int. J. of Digital Earth* **9** 113–33

[30] Pekel J F, Cottam A, Gorelick N and Belward A S 2016 High-resolution mapping of global surface water and its long-term changes *Nature* **540** 418

[31] Falkenmark and Rockström J 2004 *Balancing Water for Humans and Nature: the New Approach in Ecohydrology* (United Kingdom: Earthscan)

[32] Assouline S, Narkis K and Or D 2010 Evaporation from partially covered water surfaces *Water Resour. Res.* **46** W10539

[33] Aminzadeh M, Lehmann P and Or D 2018 Evaporation suppression and energy balance of water reservoirs covered with self-assembling floating elements *Hydrology and Earth Sys. Sci.* **22** 4015–32

[34] Trabucco A and Zomer R J 2009 CGIAR Consortium for Spatial Info.Global potential evapo-transpiration (Global-PET) and global aridity index (Global-Aridity) Geo-DatabaseAvailable online from the CGIAR-CSI GeoPortal

[35] Trabucco A and Zomer R J 2019 Global aridity index and potential evapotranspiration (ET0) Climate Database v2. figshare. Fileset (<https://doi.org/10.6084/m9.figshare.7504448.v3>)

[36] Karger D N *et al* 2017 Dryad Digital Repos.Data from: climatologies at high resolution for the Earth's land surface areas (<https://doi.org/10.5061/dryad.kd1d4>)

[37] Bontemps S *et al* 2013 Consistent global land cover maps for climate modelling communities: current achievements of the ESA's land cover CCI *Proc. of the ESA Living Planet Symp. (Edinburgh)* pp 9–13

[38] Lehner B and Döll P 2004 Development and validation of a global database of lakes, reservoirs and wetlands *J. of Hydrology* **296** 1–22

[39] Gal L, Grippa M, Hiernaux P, Peugeot C, Mougin E and Kerfoot L 2016 Changes in lakes water volume and runoff over ungauged Sahelian watersheds *J. of Hydrology* **540** 1176–88

[40] Alazard M, Leduc C, Travi Y, Boulet G and Salem A B 2015 Estimating evaporation in semi-arid areas facing data scarcity: example of the El Haouareb dam (Merguellil catchment, Central Tunisia) *J. of Hydrology: Regional Studies* **3** 265–84

[41] Vote C, Eberbach P, Inthavong T, Lampayan R M, Vongthilard S and Wade L J 2019 Quantification of an overlooked water resource in the tropical rainfed lowlands using RapidEye satellite data: a case of farm ponds and the potential gross value for smallholder production in southern Laos *Agri. Water Mgt.* **212** 111–8

[42] Rosenberry D O, Winter T C, Buso D C and Likens G E 2007 Comparison of 15 evaporation methods applied to a small mountain lake in the northeastern USA *J. of Hydrology* **340** 149–66

[43] McJannet D L, Cook F J and Burn S 2013 Comparison of techniques for estimating evaporation from an irrigation water storage *Water Resources Res.* **49** 1415–28

[44] Allen R G, Pereira L S, Raes D and Smith M 1998 Crop evapotranspiration-guidelines for computing crop water requirements-FAO irrigation and drainage paper 56 *Fao, Rome* **300** D05109

[45] Kohli A and Frenken K 2015 Evaporation from artificial lakes and reservoirs *FAO-Aquastat, Rome*

[46] Lehmann P, Aminzadeh M and Or D 2019 Evaporation suppression from water bodies using floating covers: laboratory studies of cover type, wind and radiation effects *Water Resources Res.* **55** 4839–53

[47] Center for International Earth Science Information Network—CIESIN—Columbia University. 2018 Gridded Population of the World, Version 4 (GPWv4): Population Count, Revision 11. *Palisades, NY: NASA Socioeconomic Data and Applications Center (SEDAC)* Accessed 27 Oct. 2019 (<https://doi.org/10.7927/H4JW8BX5>)